Decoherence in Josephson Phase Qubits from Junction Resonators

R. W. Simmonds, K. M. Lang, D. A. Hite, S. Nam, D. P. Pappas, and John M. Martinis*

National Institute of Standards and Technology, 325 Broadway, Boulder, Colorado 80305-3328, USA
(Received 12 September 2003; published 12 August 2004)

Although Josephson junction qubits show great promise for quantum computing, the origin of dominant decoherence mechanisms remains unknown. Improving the operation of a Josephson junction based phase qubit has revealed microscopic two-level systems or resonators within the tunnel barrier that cause decoherence. We report spectroscopic data that show a level splitting characteristic of coupling between a two-state qubit and a two-level system. Furthermore, we show Rabi oscillations whose "coherence amplitude" is significantly degraded by the presence of these spurious microwave resonators. The discovery of these resonators impacts the future of Josephson qubits as well as existing Josephson technologies.

Josephson junctions are good candidates for quantum computing [1], with recent experiments demonstrating reasonably long coherence times, state preparation, manipulation, and measurement, and the coupling of qubits for eventual gate operations [2–7]. Josephson quantum bits (qubits) may be considered as nonlinear LC resonators formed by the Josephson inductance and capacitance of a tunnel junction [4]. Making qubits from such electrical elements is advantageous because coupling of qubits and scaling to large numbers should be relatively straightforward using integrated-circuit fabrication technology. Although circuits have been invented to decouple the qubit from unwanted electromagnetic modes, solid-state systems are inherently complex and may contain defects that degrade the coherence. A full knowledge of the system's Hamiltonian requires probing the operational space of the qubit and investigating all decoherence behavior.

Here we report the discovery of spurious microwave resonators that reside within the Josephson tunnel barrier used to form a solid-state qubit. We show that at certain bias points, strong coupling to these resonators destroys the coherence of the qubit. Although previous reports have focused on the characteristic decay *time* of coherent oscillations, our data demonstrate that decoherence from these spurious resonators primarily affects the *amplitude* of the oscillations. We present a model that explains these resonators as being produced by fluctuations in the tunnel barrier. This phenomena can be compared with previous measurements of both junction current-voltage characteristics and low frequency $1/f$ critical-current noise. Although two-level systems are known to exist in amorphous materials [8], the sensitivity of our Josephson qubit at the quantum level has allowed us to uncover individual two-level microwave resonators hidden within a 40-year-old technology. As major sources of decoherence, they play a vital role in understanding the full effective Hamiltonian of Josephson tunnel junctions.

The circuit used in this experiment, shown in Fig. 1(a), is cooled to 20 mK. The junction is isolated from dissipation of the leads in a similar manner to a phase qubit described previously [4]. The circuit has been improved by placing the junction in a superconducting loop of inductance L to minimize the voltage and thus the generation of quasiparticles and self-heating when the qubit state is measured [9]. The junction is biased with current I close to the critical-current I_0 by coupling magnetic flux through a transformer with mutual inductance M. As shown in Fig. 1(b), the qubit states are formed in a cubic potential of the left well and are measured by tunneling to states in the right well. Tunneling to the right well changes the flux through the loop by $\sim \Phi_0 = h/2e$, which
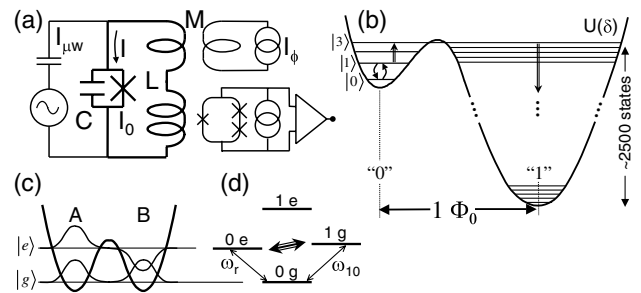

FIG. 1. (a) Circuit diagram for the Josephson junction qubit. Junction current bias I is set by I_ϕ and microwave source $I_{\mu w}$. Parameters are $I_0 \simeq 11.659$ μA, $C \simeq 1.2$ pF, $L \simeq 168$ pH, and $L/M \simeq 81$. (b) Potential energy diagram of qubit, showing qubit states $|0\rangle$ and $|1\rangle$ in cubic well at left. Measurement of $|1\rangle$ state performed by driving the $1 \rightarrow 3$ transition, tunneling to right well, then relaxation of state to bottom of right well. Postmeasurement classical states "0" and "1" differ in flux by Φ_0, which is readily measured by readout SQUID. (c) Schematic description of tunnel-barrier states A and B in a symmetric well. Tunneling between states produces ground $|g\rangle$ and excited $|e\rangle$ states separated in energy by $\hbar \omega_r$. (d) Energy-level diagram for coupled qubit and resonant states for $\omega_{10} \simeq \omega_r$. Coupling strength between states $|1g\rangle$ and $|0e\rangle$ is given by $\bar{H}_{int}$.

is easily read out with a pulsed critical-current measurement in a separate SQUID detector. The qubit was fabricated using aluminum metallization, with an aluminum-oxide tunnel barrier formed by an ion-mill clean followed by thermal oxidation [9].

The $0 \rightarrow 1$ qubit transition frequency ω_{10} is measured spectroscopically [10], as shown in Fig. 2(a). For our measurements, the current bias is pulsed for a time $\sim 50 \ \mu$s to a value close enough to the critical current so that approximately 3–4 energy levels are in the cubic well. Transition frequencies are probed by applying microwave current $I_{\mu w}$ at frequency ω and measuring a resonant increase in the net tunneling probability. We observe in Fig. 2(a) a decrease in the transition frequency as the bias current approaches the critical current, as expected theoretically for the ω_{10} transition.

Additionally, we observe a number of small spurious resonators (indicated by dotted vertical lines) that are

characteristic of energy-level repulsion predicted for coupled two-state systems. These extra resonators have a distribution in splitting size, with the largest one giving a splitting of ~ 25 MHz and an approximate density of 1 major spurious resonator per ~ 60 MHz.

We observed coherent "Rabi oscillations" between the $|0\rangle$ and the $|1\rangle$ states by pulsing microwaves at the $0 \rightarrow 1$ transition frequency ω_{10}, then measuring the occupation probability of state $|1\rangle$ by applying a second microwave pulse resonant with the $1 \rightarrow 3$ transition frequency ω_{31} [4]. Figures 3(a)–3(c) show for three values of microwave power the occupation probability versus the Rabi-pulse time t_r at a bias point away from any resonators. The decay of the oscillations is approximately exponential and gives a coherence time of 41 ns. Figure 3(d) shows that the oscillation frequency is proportional to the microwave amplitude, as expected.

The correlation between Rabi oscillations and spurious resonators is demonstrated in Fig. 2. For the data in Fig. 2(b), the microwave frequencies of the Rabi and measurement pulses were adjusted with I to center on the transition frequencies obtained from spectroscopy data. We observe that the oscillation amplitude, represented by a variation in color, is suppressed over time (vertical axis) at particular bias currents (horizontal axis). The dashed vertical lines show that this suppression is correlated to those transition frequencies ω_{10} where there are pronounced resonator structures. It is clear that these spurious resonators strongly disrupt the Rabi oscillations.

In Fig. 4 we show the decay of the Rabi oscillations for biases indicated by arrows in Fig. 2(b). Near resonators we find unusual behavior such as beating [4(b)], loss and recovery of the oscillations with time [4(c)], and rapid loss of coherence amplitude [4(f)]. The general trend is
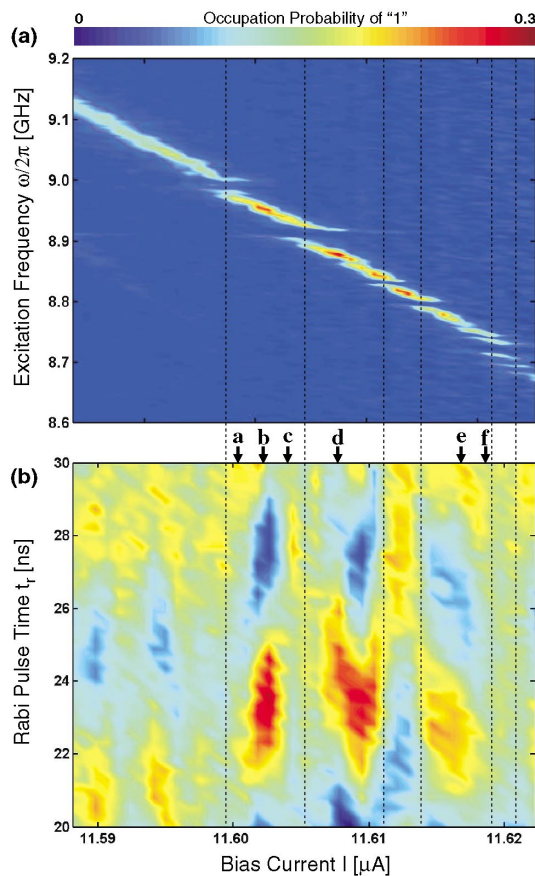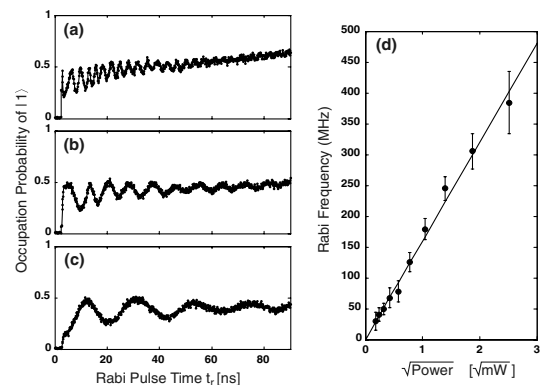

FIG. 2 (color). (a) Measured probability of state "1" versus microwave excitation frequency $\omega/2\pi$ and bias current I for a fixed microwave power. Data indicate ω_{10} transition frequency. Dotted vertical lines are centered at spurious resonators. (b) Measured occupation probability of $|1\rangle$ versus Rabi-pulse time t_r and bias current I. In (b), a color change from dark blue to red corresponds to a probability change of 0.4. Color modulation in time t_r (vertical direction) indicates Rabi oscillations.

FIG. 3. (a)–(c) Measured occupation probability of $|1\rangle$ versus time duration of Rabi pulse t_r for three values of microwave power, taken at bias $I = 11.609 \ \mu$A in Fig. 2. The applied microwave powers for (a), (b), and (c) correspond to 0.1, 0.33, and 1.1 mW, respectively. (d) Plot of Rabi oscillation frequency versus microwave amplitude. A linear dependence is observed, as expected from theory.
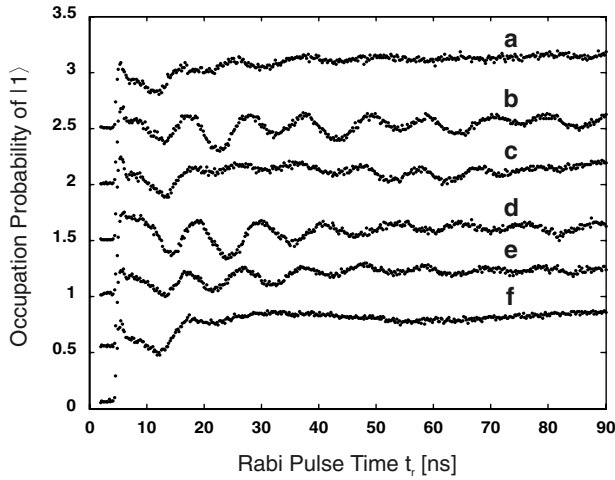
FIG. 4. Measured occupation probability of $|1\rangle$ versus time duration of Rabi pulse t_r for current biases (a)–(f) as noted by arrows in Fig. 2. Data (a)–(e) are offset for clarity. Note that when the bias is changed, the coherence is degraded mainly as a loss in amplitude, not by a decrease in coherence time.

that spurious resonators cause loss in coherence not by a decrease in the decay time of the oscillations, but by a decrease in the amplitude of the oscillations.

Experimental checks were performed to rule out whether these resonators arise from coupling to the read-out SQUID or modes in the device mount [11]. Additionally, simulations show that the beating behavior in Fig. 4 is consistent with the interaction of the qubit with another two level system but not harmonic oscillator modes from the leads of the device. When thermally cycled to room temperature, the magnitude and frequency of the spurious resonators can change considerably, whereas cycling to 4 K produces no apparent effect. Furthermore, for the same experimental setup and over ten qubit devices, we find that each qubit has its own unique "fingerprint" of resonator frequencies and splitting strengths. Finally, over many hours while the device is cold, we observe that resonator frequencies and strengths can change spontaneously. All of these observations indicate that the resonators are microscopic in origin.

We have constructed a model for the microscopic resonators, where we consider two-level states in the barrier with large tunneling matrix elements corresponding to a microwave frequency [12]. If we consider two states in the tunnel barrier that have configurations A and B producing critical currents I_{0A} and I_{0B}, then the interaction Hamiltonian between the resonator and the critical-current is

$$
H_{\rm int} = -\frac{I_{0A}\Phi_0}{2\pi}\cos\hat{\delta} \otimes |\Psi_A\rangle\langle\Psi_A|
$$
$$
\qquad -\frac{I_{0B}\Phi_0}{2\pi}\cos\hat{\delta} \otimes |\Psi_B\rangle\langle\Psi_B|, \qquad (1)
$$

where $\hat{\delta}$ is an operator corresponding to the phase difference across the junction, and $\Psi_{A,B}$ describe the two wave functions for two configuration states of a resonator within the tunnel barrier. If we assume a symmetric potential with energy eigenstates separated by $\hbar\omega_r$, the ground and excited states are given by $|g\rangle \simeq (|\Psi_A\rangle + |\Psi_B\rangle)/\sqrt{2}$ and $|e\rangle \simeq (|\Psi_A\rangle - |\Psi_B\rangle)/\sqrt{2}$. Because the junction is biased near its critical current, $\delta \to \delta + \pi/2$ with $\delta \ll 1$, we take $\cos\hat{\delta} \to \hat{\delta}$. Using matrix elements appropriate for the phase qubit [14] and including only the dominant resonant terms arising from this interaction Hamiltonian, we find

$$
\tilde{H}_{\rm int} = \frac{\Delta I_0}{2}\sqrt{\frac{\hbar}{2\omega_{10}C}}(|0\rangle\langle1| \otimes |e\rangle\langle g| + |1\rangle\langle0| \otimes |g\rangle\langle e|),
$$

where $\Delta I_0 = I_{0A} - I_{0B}$. Figure 1(d) shows an energy level diagram for the case where $\omega_r \approx \omega_{10}$. The coupling of the two intermediate energy levels through $\tilde{H}_{\rm int}$ produces a repulsion in the energy eigenstates that corresponds to the spectroscopic data in Fig. 2(a). From the magnitude of level repulsions on resonance, the largest value being $2|\tilde{H}_{\rm int}|/h \simeq 25$ MHz, we obtain from our model $(\Delta I_0/I_0)_{\rm res} \lesssim 65 \times 10^{-6}$.

If we assume that the two configurations A and B correspond to turning on and off an individual conduction channel in the tunnel barrier, then $(\Delta I_0/I_0)$ can be estimated from the current-voltage characteristics of the junction. For a nonuniform tunnel barrier, mesoscopic theory [15] predicts that the total current flowing through a junction comes from a sum over a number of conduction channels with tunneling transmissions τ_i. These transmission coefficients can be measured from steps in the subgap current-voltage characteristics [16]. These steps have magnitude $2/\tau_i$ and arise from nth order multiple Andreev reflections at subharmonic gap voltages $2\Delta/en$. If we assume the current is carried by $N_{\rm ch}$ channels, each with an average transmission τ, then our measured current-voltage characteristics [9] imply $\tau \approx 4 \times 10^{-3}$ for a critical-current density of ~ 40 A/cm². For our qubit junction with a normal-state resistance $R_N = 29$ Ω, we calculate that the average fraction of the critical current carried by each channel is roughly $(\Delta I_0/I_0)_{I\text{-}V} = 1/N_{\rm ch} = 2\tau R_N e^2/h \simeq 8 \times 10^{-6}$. This value is in reasonable agreement with those obtained from the magnitudes of the resonator splittings considering that the junction has a distribution of tunneling transmissions τ_i and our measurements of the level repulsions identify only a small fraction of the largest resonators from their full distribution.

We can also compare these results with $1/f$ critical-current noise measurements at audio frequencies for individual $1/f$ fluctuators within submicrometer junctions [13,17,18]. For an aluminum junction with area 0.08 μm², a single fluctuator [13] gave a change in critical current of $\Delta I_0 \simeq 10^{-4} I_0$. Scaling this fractional change to our qubit

junction with an area of 32 μm^2, we obtain $(\Delta I_0/I_0)_{1/f} \simeq 0.3 \times 10^{-6}$ for a single fluctuator, about 30 times smaller than estimated above from the current-voltage characteristics. A factor of ~ 4 in this ratio is due to enhanced subgap current arising from surface inhomogeneities created by an ion-mill cleaning step in our junction fabrication process. Additionally, the density of fluctuators in frequency may also be compared. Several experiments give approximately one resonator per decade in frequency for junctions with area 0.1 μm^2 [13,17], which is higher by only a factor of 2 than the areal density we observed for the resonators at microwave frequencies.

The magnitude and density in frequency of the microwave resonators and low frequency $1/f$ noise fluctuators are in reasonable agreement, especially since they compare phenomena that have characteristic frequencies separated by many orders of magnitude. With good agreement between the resonator model, our data, and data from $1/f$ noise, it seems plausible that junctions with low $1/f$ noise will contain weaker spurious microwave resonators. This suggests that we can estimate from previous $1/f$ measurements the performance of qubits using alternative materials. A recent compilation of $1/f$ noise data indicates that tunnel junctions made from oxides of Al, Nb, and In all have similar magnitudes of noise [13]. This evidence suggests that alternatives to simple thermal or plasma oxidation of metals should be investigated.

In conclusion, we have developed an improved Josephson-phase qubit whose sensitivity at the quantum level has allowed the discovery of spurious microwave resonators within Josephson tunnel junctions. We have observed a strong correlation between these resonators and decoherence in the qubit, showing that they primarily degrade the coherence of Rabi oscillations through a reduction of the "coherence amplitude." These resonators can be modeled as arising from two-level states within the tunnel barrier, which couple to the qubit's states through the critical current. This represents a new term in the Hamiltonian of fabricated Josephson tunnel junctions that has remained hidden for over 40 years. These microwave resonators may be affecting the performance of existing Josephson technologies. Furthermore, we predict that improvements in the coherence of all Josephson qubits will require materials research directed at redistributing, reducing, or removing these resonator states.

---

*Electronic address: martinis@physics.ucsb.edu

[1] M. A. Nielsen and I. L. Chuang, *Quantum Computation and Quantum Information* (Cambridge University Press, Cambridge, 2000).

[2] D. Vion, A. Aassime, A. Cottet, P. Joyez, H. Pothier, C. Urbina, D. Esteve, and M. H. Devoret, Science **296**, 886 (2002).

[3] Y. Yu, S. Han, X. Chu, S. Chu, and Z. Wang, Science **296**, 889 (2002).

[4] J. M. Martinis, S. Nam, J. Aumentado, and C. Urbina, Phys. Rev. Lett. **89**, 117901 (2002).

[5] I. Chiorescu, Y. Nakamura, C. J. P. M. Harmans, and J. E. Mooij, Science **299**, 1869 (2003).

[6] Yu. A. Pashkin, T. Yamamoto, O. Astafiev, Y. Nakamura, D. V. Averin, and J. S. Tsai, Nature (London) **421**, 823 (2003).

[7] A. J. Berkley, H. Xu, R. C. Ramos, M. A. Gubrud, F. W. Strauch, P. R. Johnson, J. R. Anderson, A. J. Dragt, C. J. Lobb, and F. C. Wellstood, Science **300**, 1548 (2003).

[8] W. A. Phillips, Rep. Prog. Phys. **50**, 1657 (1987).

[9] K. M. Lang, S. Nam, J. Aumentado, C. Urbina, and J. M. Martinis, IEEE Trans. Appl. Supercond. **13**, 989 (2003).

[10] J. M. Martinis, M. H. Devoret, and J. Clarke, Phys. Rev. Lett. **55**, 1543 (1985).

[11] The frequencies of resonant modes in our mounting box are consistent with its dimensions, and are not correlated with the spurious resonators. Additionally, the resonator frequency of the measurement SQUID depends on its bias current—no change in the frequencies of spurious resonators was observed as this bias was varied.

[12] Critical-current fluctuations are often depicted as arising from trapping of electrons in the barrier (see, for example, Ref. [13]). With experimental data showing nonuniform barriers and no qualitative change in the $1/f$ noise below T_c, we believe our tunneling-channel model is more physically realistic.

[13] For several different types of junctions with area A, critical-current spectral density S_{I_o}, and critical current I_o, the quantity $\sqrt{AS_{I_o}}/I_o$ at 4.2 K varies by less than a factor of 3. The data are from B. Savo, F. C. Wellstood, and J. Clarke, Appl. Phys. Lett. **50**, 1757 (1987); V. Foglietti, W. F. Gallagher, M. B. Ketchen, A. W. Kleinsasser, R. H. Koch, S. I. Raider, and R. L. Sandstrom, Appl. Phys. Lett. **49**, 1393 (1986); R. H. Koch, D. J. V. Harlingen, and J. Clarke, Phys. Rev. B **26**, 74 (1982); and was compared by D. J. VanHarlingen, B. L. T. Plourde, T. L. Robertson, P. A. Reichardt, and J. Clarke (see cond-mat/0404307).

[14] J. M. Martinis, S. Nam, J. Aumentado, K. M. Lang, and C. Urbina, Phys. Rev. B **67**, 094510 (2003).

[15] E. N. Bratus, V. S. Shumeiko, and G. A. B. Wendin, Phys. Rev. Lett. **74**, 2110 (1995); D. Averin and A. Bardas, Phys. Rev. Lett. **75**, 1831 (1995); C. W. J. Beenakker, Phys. Rev. Lett. **67**, 3836 (1991).

[16] N. van der Post, E. T. Peters, I. K. Yanson, and J. M. van Ruitenbeek, Phys. Rev. Lett. **73**, 2611 (1994); M. F. Goffman, R. Cron, A. Levy Yeyati, P. Joyez, M. H. Devoret, D. Esteve, and C. Urbina, Phys. Rev. Lett. **85**, 170 (2000).

[17] C. T. Rogers and R. A. Buhrman, Phys. Rev. Lett. **53**, 1272 (1984); **55**, 859 (1985).

[18] R. T. Wakai and D. J. VanHarlingen, Appl. Phys. Lett. **49**, 593 (1986).